Molecular Crystals and Liquid Crystals Incorporating Nonlinear Optics

Publication details, including instructions for authors and subscription information:
http://www.tandfonline.com/loi/gmcl17

Molecular Dynamics Simulations of Phenyl-4-(4-benzoyloxy-)benzoyloxy-benzoate in the Crystalline and Nematic Phase

B. Jung [a] & B. L. Schürmann [a]

[a] Max-Planck-Institut für Polymerforschung, Postfach 3148, D-6500, Mainz, Germany

Version of record first published: 22 Sep 2006.

To cite this article: B. Jung & B. L. Schürmann (1990): Molecular Dynamics Simulations of Phenyl-4-(4-benzoyloxy-)benzoyloxy-benzoate in the Crystalline and Nematic Phase, Molecular Crystals and Liquid Crystals Incorporating Nonlinear Optics, 185:1, 141-153

To link to this article: http://dx.doi.org/10.1080/00268949008038497

Mol. Cryst. Liq. Cryst., 1990, Vol. 185, pp. 141–153
Reprints available directly from the publisher
Photocopying permitted by license only

Printed in the United States of America

Molecular Dynamics Simulations of Phenyl-4-(4-benzoyloxy-)benzoyloxybenzoate in the Crystalline and Nematic Phase

B. JUNG and B. L. SCHÜRMANN

Max-Planck-Institut für Polymerforschung, Postfach 3148, D-6500 Mainz, Germany

(*Received January 10, 1990*)

A model of the crystal structure of phenyl-4-(4-benzoyloxy-)benzoyloxybenzoate has been created by a sequence of forcefield prior to molecular dynamics calculations. The simulated x-ray powder diagram shows good agreement with the experimental diffractrogram. Investigation on the nematic phase on the all atom level by Molecular Dynamics computer simulation describes characteristic motions of the molecules in this type of liquid crystals.

I. INTRODUCTION

One of the interesting aspects of "stiff-molecules" is the fact that they can appear in different phases, i.e. crystalline, smectic, nematic, and isotropic. An oligomer which serves as a model for the entire class of linear polymers with rod-like main chain forming a crystalline, nematic and isotropic phase is (phenyl-4-(4-benzoyloxy-)benzoyloxy benzoate (see Figure 1). It may be considered as a segment of the liquid crystalline polyester poly(p-oxy benzoate) (pHB) and will be called "tetramer" in the following text.[1]

Extending our previous work on the theoretical investigation of the intrinsic stiffness of pHB by molecular dynamics simulations of a single chain in vacuo[2,3] we will now consider a system of densely packed short chains, i.e. the "tetramer" of pHB. The system consists of the tetramer molecules which will be investigated under the conditions of an NVT-ensemble. (In a NVT-ensemble, the number of atoms, the volume and the temperature are kept constant.)

Our motivation to choose the tetramer shown by Figure 1 is twofold:

—The x-ray powder diagram[4] of the tetramer was available to us from which the size of the unit cell could be derived. Based on this information we could try to use the molecular dynamics method to find stable conformations in the conformational space by tuning the temperature as a driving parameter to overcome potential barriers.

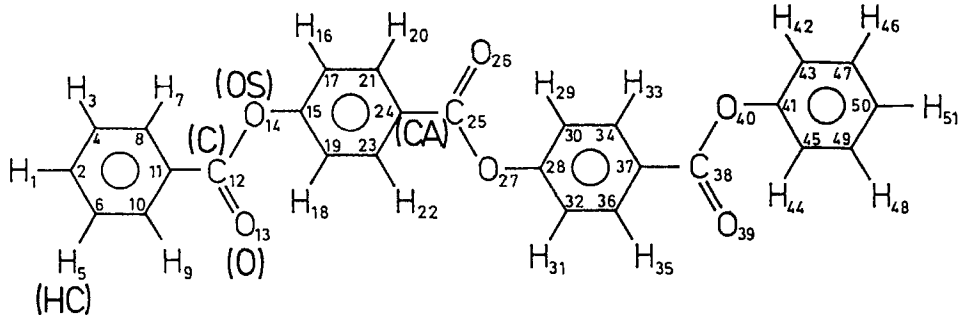

FIGURE 1 Tetramer with symbolic names (phenyl-4-(4-benzoyloxy-)benzoyloxy benzoate.

—We wanted to learn whether the molecular dynamics method can be applied to develop a realistic description of the nematic phase and the molecular motions in the course of phase transitions.

We will proceed in the following way:

In section II we will introduce the molecular model and the forcefield used in the MD-simulations of the crystalline and the nematic phase. In section III we will give some details of the computational procedure. Section IV describes the simulation of the x-ray powder diagram and finally in section V we concentrate on the simulation of the nematic phase.

II. MOLECULAR MODEL

The basic equation for the forcefield is the same as used previously,[2] i.e. the standard expression for the potential energy V without the 10–12 hydrogen bond term implemented in the Amber code[5]:

$$V = \sum_b f_b(r_b - r_{b\,eq})^2 \qquad \text{bond stretching terms}$$

$$+ \sum_\nu f_\nu(\delta_\nu - \delta_{\nu\,eq})^2 \qquad \text{valence angle terms}$$

$$+ \sum_d f_d(1 + \cos(n_d \varphi_d - \delta_d) \qquad \text{dihedral angle terms} \qquad (1)$$

$$+ \sum_{i,j} \frac{1}{4\pi\epsilon} \frac{q_i q_j}{r_{ij}} \qquad \text{Coulomb terms}$$

$$+ \sum_{i,j} \frac{A_{ij}}{r_{ij}^{12}} - \frac{B_{ij}}{r_{ij}^{6}} \; (i < j) \qquad \text{Lennard-Jones terms}$$

The van der Waals parameters are calculated by the Slater-Kirkwood rule

$$A_{ij} = \epsilon_{ij}^{*} \cdot r_{ij}^{12}$$
$$B_{ij} = 2\,\epsilon_{ij}^{*} \cdot r_{ij}^{6} \tag{2}$$

with

$$\epsilon_{ij}^{*} = \sqrt{\epsilon_i^{*} \cdot \epsilon_j^{*}} \tag{3}$$

$$r_{ij} = (r_i^{*} + r_j^{*}) \tag{4}$$

Here ϵ_i^{*}, ϵ_j^{*} are the potential well depths and r_i, r_j are the van der Waals-radii of the respective atoms. The assignment of the symbolic names of the molecular structure of the "tetramer" together with the assignments of the various atoms, bonds and groups is displayed in Figure 1. In contrast to our previous calculations we work now on the "all atom" level, since in dense systems the H-atoms need explicitly to be taken into account because of space filling arguments and the more detailed charge distribution. The forcefield parameters required for the potential energy terms (1) are given in Table I. These numerical values are averages derived from data of microwave spectroscopy, neutron diffraction, NMR studies and quantum mechanical calculations. The partial charges were calculated by the MNDO method, they are given in Table II.

We knew from the experimental x-ray powder diagram that there were 4 molecules in an orthogonal unit cell of the size 0.75 × 0.55 × 4.92 nm. The box size chosen for our simulation was twice the size of the unit cell (0.75 × 4.92 × 1.11 nm) and 8 molecules were packed in the way that the longest molecular axis was parallel to the *y*-axis.

Each molecule was treated separately to find the local minimum for the most stable conformation using the steepest descent method of the Amber code.

In each molecule the first and third carbonyl group were in the same place and two benzene rings in one molecule formed an angle of 90°.

The knowledge of the size of the unit cell still leaves some freedom for different packing arrangements, the only restriction is that within our box two identical unit cells are supposed to be in *z*-direction. Within this framework we made three initial guesses for the crystal structure which were minimized with respect to their inter- and intramolecular interactions. The cutoff radius limiting the number of interacting pairs was fixed to be half of the smallest box dimension:

Model I) Four molecules were put in one layer in parallel manner, i.e. the carbonyl-oxygens were pointing in the same direction. In the second layer the molecules were antiparallel with respect to the ones in the first layer.

Model II) The molecules in the same layer were antiparallel to each other. The second layer was identical to the first one.

Model III) All the 8 molecules were pointing in the same direction.

TABLE I

Forcefield parameters for phenyl-4-(4-benzoyloxy-)benzoyloxybenzoate

Bonding potential parameters:

	f_b [kcal/mol]	$r_{b\,eq}$ [Å]
C—CA	469.0	1.40
C—O	570.0	1.23
C—OS	520.0	1.36
CA—CA	469.0	1.40
CA—OS	520.0	1.37
CA—HC	340.0	1.08

Valence angle parameters:

	f_v [kcal/rad^2]	$\varphi_{v\,eq}$ [degrees]
CA—C—O	80.0	120.0
O—C—OS	80.0	126.0
CA—C—OS	90.0	111.8
CA—CA—CA	85.0	120.0
CA—CA—HC	35.0	120.0
OS—CA—CA	70.0	120.0
C—CA—CA	85.0	120.0
CA—OS—C	80.0	120.0

Dihedral angle parameters:

	f_d [kcal]	δ_d [degrees]	n_d
—CA—OS—	4.0	0.0	2
—C—CA—	8.0	180.0	2
—C—OS—	10.0	180.0	2
—CA—CA—	5.3	180.0	2
Improper dihedral angles:			
O—C—	10.5	180.0	2
OS—CA—	10.0	180.0	2
C—CA—	10.0	180.0	2
HC—CA—	2.0	180.0	2

(Improper dihedral angles are used to keep the ester bonds and the substituents at the benzene ring in plane.)

Van der Waals parameter:

	Van der Waals radius [Å]	potential well depth [kcal]
OS	1.65	0.15
O	1.60	0.20
C	1.85	0.12
CA	1.85	0.12
HC	1.54	0.01

TABLE II

Partial charges: (The indices correspond to those in figure 1.)

q_1	0.083	q_{20},q_{22},q_{33},q_{35}	0.117
q_2	−0.023	q_{21},q_{23},q_{34},q_{36}	0.056
q_3,q_5	0.089	q_{24},q_{37}	−0.155
q_4,q_6	−0.112	q_{25},q_{38}	0.545
q_7,q_9	0.101	q_{26},q_{39}	−0.480
q_8,q_{10}	0.013	q_{40}	−0.375
q_{11}	−0.146	q_{41}	0.137
q_{12}	0.536	q_{42},q_{44}	0.092
q_{13}	−0.461	q_{43},q_{45}	−0.077
q_{14},q_{27}	−0.401	q_{46},q_{48}	0.081
q_{15},q_{28}	0.251	q_{47},q_{49}	−0.064
q_{16},q_{18},q_{29},q_{31}	0.107	q_{50}	−0.079
q_{17},q_{19},q_{30},q_{32}	−0.160	q_{51}	0.082

After the minimization a short molecular dynamics run of 1.5 ps at 100 K was performed to relax the arrangement of the configuration. Then again these structures were minimized. It turned out that model III was energetically favoured.

III. COMPUTATIONAL PROCEDURE (DETAILS)

A local minimum of the potential energy hypersurface after the minimization is found in the sense that unreasonable contacts of the particles are not existent. This structure is then taken as initial conformation for the simulation of the molecular dynamics with periodic boundary conditions and coupling to a heat bath.[6] The volume of the box is held constant, i.e. we used the NVT-ensemble. Each particle of the system is perturbed by an amount of kinetic energy due to a Maxwell distribution.

$$\frac{3}{2} KT = \frac{1}{2} mv^2 \tag{4}$$

To avoid high initial velocities the temperature T is chosen to be 10 K. After having removed the center of mass velocity and angular momentum of the whole system and having received the set of velocities we applied the "leap-frog"[7] algorithm to create the trajectory $\vec{x}\ (t + dt)$ and $\vec{v}\ (t + dt/2)$.

$$\vec{x}_i\ (t + dt) = \vec{x}_i\ (t) + \vec{v}_i \left(t + \frac{dt}{2}\right) dt \tag{5}$$

$$\vec{v}_i \left(t + \frac{dt}{2}\right) = \vec{v}_i \left(t - \frac{1}{2} dt\right) + \frac{\vec{F}_i}{m_i} dt \tag{6}$$

The time steps dt were 0.0005 ps. There were no constraints incorporated on any possible bond distortions or vibrations. The force in Equation (6) is obtained from

the Newtonian equation

$$\vec{F}_i = m_i\vec{a}_i = -\frac{\partial V}{\partial \vec{x}_i} \tag{7}$$

$\vec{x}_i$, $\vec{v}_i$, $\vec{a}_i$, m_i, $\vec{l}_i$ are position, velocity, acceleration and mass of the atom i and the force acting on the atom i. The coupling to a heat bath requires scaling of the velocities with regard to temperature and time

$$v(t) = v(t)\left(1 + \frac{1}{T}\frac{T_o - T}{\tau_T}\Delta t\right)^{\frac{1}{2}} \tag{8}$$

The change of the temperature T is considered as relaxation of first order. T_o is the reference temperature of the heat bath and τ_T is the coupling constant chosen to be 0.05 ps in our simulations.

In the framework of these algorithms the molecular dynamics simulation was allowed to run at 300 K for 70 ps. The cutoff radius for the non bonded interactions was taken to be 3.75 nm. After 70 ps the potential energy was quasi stable (fluctuations ca. 12 kcal), so we accepted this averaged structure as the crystal structure.

In comparison to the initial structure the molecules were slightly tilted and the angle between two benzene rings in sequence was decreased to be 65° while the carbonyl groups were slightly rotated out of the plane of the adjacent benzene ring. This phenomenon is already known from related crystal structures[8] and agrees well with the interpretation of the x-ray diffraction results of Coulter.[9]

The modelled crystal structure is pictured in Figure 2.

IV. SIMULATION OF THE X-RAY POWDER DIAGRAM

We calculated the scattering intensity according to[10]

$$I(hkl) = P{\cdot}L{\cdot}|F|^2 \tag{9}$$

with

P polarization factor giving the loss due to the polarization of the scattered light $P = (1 + \cos^2 2\Theta)/2$

L $= 1/(\sin 2\Theta{\cdot}\sin\Theta)$
Lorentz factor

The scattering angle 2Θ is correlated to the wave length λ (in this case λ (Cu-K_α) = 1.5418 Å) of the x-ray source and to the distance of the lattice planes by Bragg's law

$$\sin\Theta = \lambda/2d \tag{10}$$

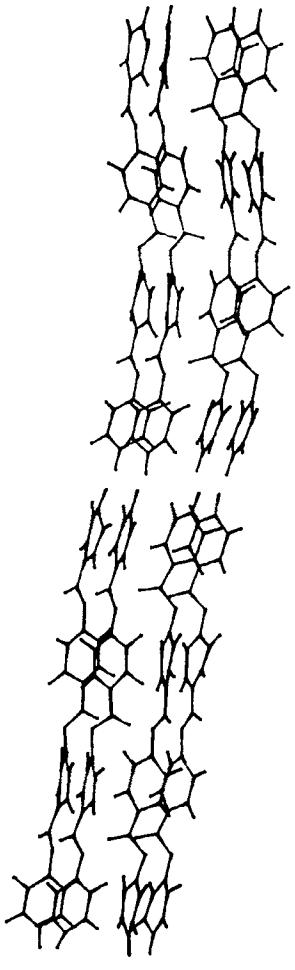

FIGURE 2 The crystal structure created by MD-simulations of the tetramer.

The effect of the temperature was taken into account by the Debye-Waller factor M_n; $\langle\mu_n^2\rangle$ is the mean squared deviation of the nth atom from its mean position

$$M_n = \exp\{-8\pi^2 \langle\mu_n^2\rangle (\sin^2\Theta)/\lambda^2\} \tag{11}$$

In this way we obtained a histogram, in which the peaks still needed to be convoluted by a Gaussian distribution according to

$$I(\Theta) = \sum_{hkl} I(hkl) \cdot \exp - \{(\sin\Theta_m - \sin\Theta)^2/(2\sin^2 PB)\}$$

Θ_m position of the hkl reflex (12)

PB parameter determining the width of the peak

The scattering intensity was calculated for each *hkl*-reflection within the interval $-8 \leq h,k,l \leq 8$ using the averaged atomic coordinates of each carbon- and oxygen atom from the trajectory. This trajectory was created by taking the minimized and pre-relaxed crystal structure as the initial conformation for a molecular dynamics run of 38 ps performed in the same manner as described above. The averaging of the atomic coordinates of each carbon- and oxygen atom was done for the last 33 ps of the trajectory. The mean squared deviation of each atom was in the range of 0.09 Å^2. This way we ensured ourselves to be at least close to thermal equilibrium.

Figures 3 and 4 show the calculated and the experimental x-ray powder diagram which are in good agreement. Nevertheless the remaining deviations need to be discussed:

The experimental x-ray powder diagram shows an aperiodicity of the 001-reflections: the 002-reflex occurs at 3.6°, 004 at 7.0°, 006 at 11.5° and 008 at 14.9°. The reason for this aperiodicity could be that the sample contains a kind of superstructure. Furthermore, the occurrence of another phase as an impurity would explain the additional reflection at 8.0° which cannot be indexed in the aforementioned unit cell.

The simulated powder diagram cannot display any aperiodicity in the above mentioned sense because of the periodic boundary conditions under which the simulation has been performed. The fact that the 011-reflection is found in the simulation but not in the experimental diagram is explained in the context that in

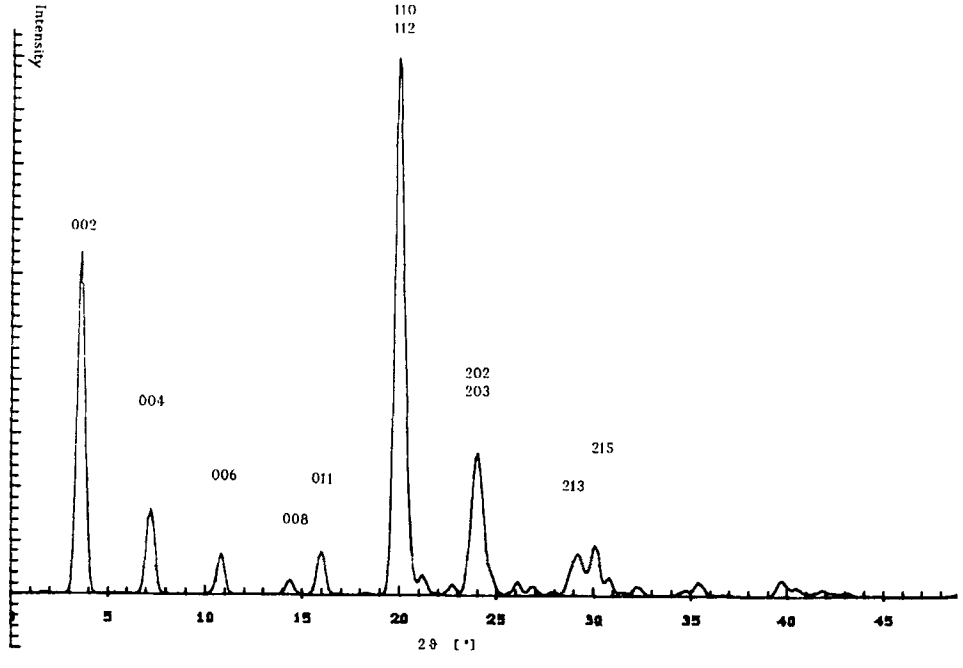

FIGURE 3 X-ray powder diagram calculated with the crystal structure obtained from MD-simulations. The indices refer to the primitive unit cell.

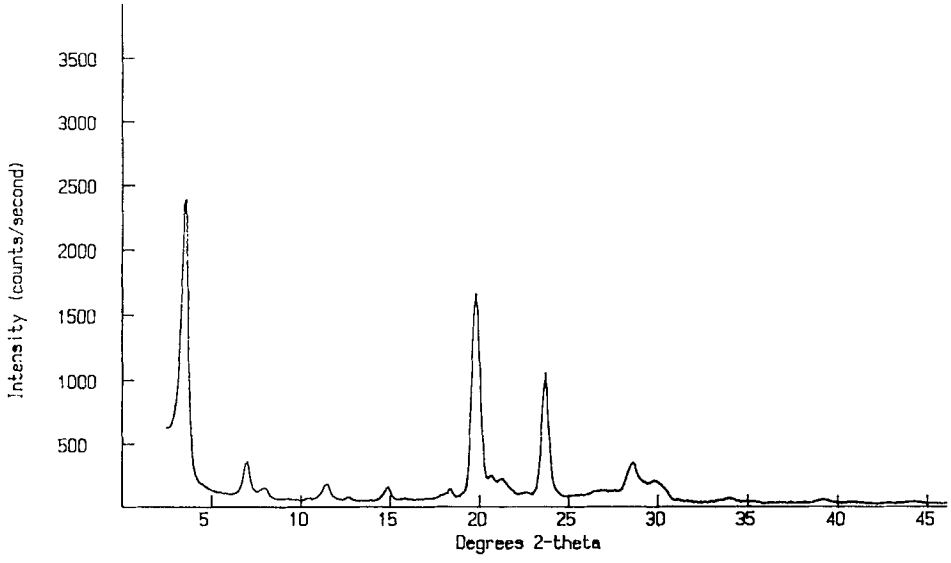

FIGURE 4 The experimental x-ray powder diagram of the tetramer.

our crystal structure there is only one position of the carbonyl-oxygen atoms with respect to the other ones per chain. In this context we like to stress clearly that the simulated diagram (Figure 3) was not fitted to the experimental result by any means, but it is the result of a quasi "ab initio" calculation based simply on the information about the size of the unit cell.

In conclusion we like to remark that the agreement between calculation and experiment is acceptable. We consider MD-calculations as a reasonable and helpful tool in the search for crystal structures in cases when single crystals are not available.

V. SIMULATION OF THE NEMATIC PHASE

For the simulation of the nematic phase of the tetramer we used the same forcefield parameters (Table I). 16 molecules were packed in 4 layers. The molecules in one layer were pointing in the same direction, two layers were rotated by 180° with respect to each other.

This system was put in a box of $20.12 \times 25.78 \times 18.98$ Å^3, which corresponds to the density of the nematic phase[1] ($\rho = 1.18$ g/cm^3). After the minimization of the potential energy a molecular dynamics simulation of 116 ps at 500 K was performed. A snapshot of the arrangement of the tetramers at 500 K is pictured in Figure 5. The cutoff radius for including the non-bonded interactions of pairs was set to be 6.5 Å. After these 116 ps the fluctuations of the temperature were within the range of 10 K, and the potential energy was stable, so we considered the system to be in thermal equilibrium.

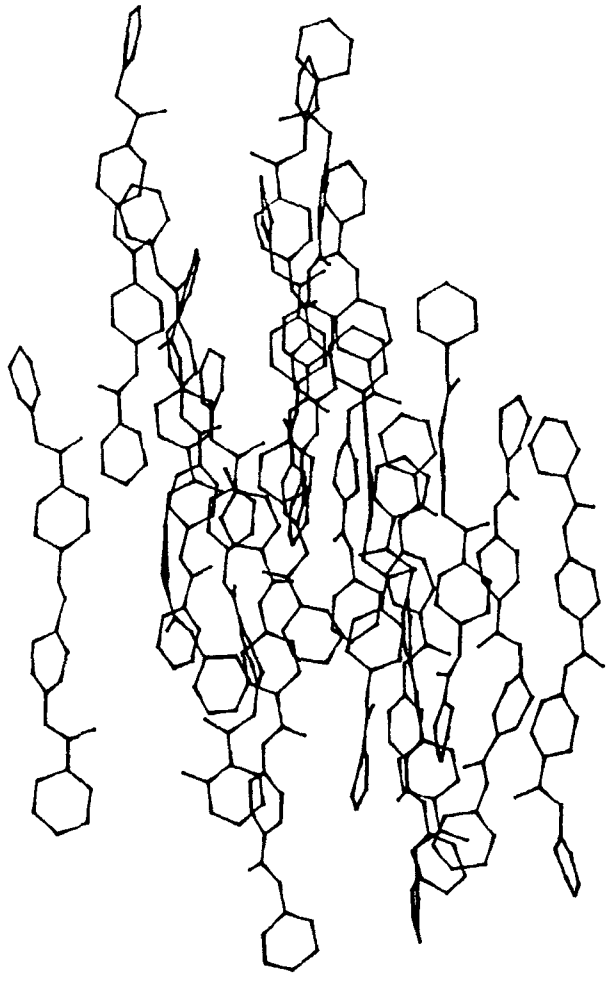

FIGURE 5 Configuration of the tetramers in the nematic phase at 500 K. The plot doesn't contain the H-atoms.

We took this structure as initial conformation for further molecular dynamics simulations of 33 ps each at different temperatures within the nematic phase and beyond (i.e. we also performed calculations for temperatures corresponding to the crystalline and isotropic phase). For each temperature 660 conformations were stored, from which 550 conformations were used for the analysis. We skipped the first 5.5 ps trajectory because the system needs to adjust to the new temperature. The coordinates were corrected with respect to the translation of the center of mass.

The translational selfdiffusion coefficient was calculated from the Einstein relation[11] for all three directions in space

$$D(\tau) = \lim_{\tau \to \infty} \frac{1}{2\tau} \langle \Delta^2 (\tau) \rangle \tag{13}$$

with

$$\Delta(\tau) = r(t) - r(t - \tau)$$

For the calculation of $\langle \Delta^2(\tau) \rangle$ only the coordinates of the carbon and oxygen atoms were taken into account. $D(\tau)$ was averaged over the trajectory for $\tau = [22.5 - 25.0]$ ps.

Before we start to interpret the results of this computer experiment we shall recall the limitations and critical aspects of the conditions under which the molecular dynamics was performed:

1. The volume of the system was held constant to maintain the density corresponding to the one found in the nematic phase at the phase transition nematic-crystalline.[1]
2. The size of the box is rather small, i.e. because of the periodic boundary conditions each atom comes pretty close to its own image. This is realistic for simulations in the crystalline phase but not for the ones in the liquid phase.
3. By the choice of this specific box each molecule is in the neighbourhood to itself in the direction of the molecular axis.
4. The time intervals followed by the simulation are too short.

The consequences of these conditions are rather obvious in the sense that we cannot expect to observe a real phase transition nematic-crystalline and nematic-isotropic. To trace on these phenomena one must allow the system to perform volume contraction and volume expansion. Also the time scale for these processes is in the order of seconds. Nevertheless, the short range effects in the nematic phase, i.e. within the temperature range 450–530 K are reliably described. In Figure 6 one detects a steep increase followed by a decrease of about the same slope for the diffusion constant along the long axis of the chain within this temperature range; there is a pronounced anisotropy.

The order of magnitude of the diffusion constant towards the long axis is the same as measured by NMR for *p*-azoxyanisole (about 10^{-9} m^2/s) and for *p*-Methoxybenzylidene-*p*-butylaniline (about 10^{-10} m^2/s).[13] It is also observed experimentally that the selfdiffusion is faster in the chain direction than in perpendicular direction, but this anisotropy is larger in the computer experiment. It is known that in different time scales different diffusion constants are measured.[13] A possible explanation for this phenomenon is given by a model for a continuous in comparison to a discrete diffusion process.[14] The latter is imagined as discrete jumps from one low energy lattice point to another. This kind of movement can be observed only on length scales bigger than the lattice constant and within large enough time scales. In our computer experiment each molecule can only see its own image along the chain direction and therefore, the whole movement is affected only by the interaction with the other molecules surrounding it normal to the long axis. To achieve a diffusion perpendicular to the long molecular axis the system needs to perform collective modes and this requires a longer simulation time.

The increase of the diffusion constant between 450–500 K refers to an increase of the kinetic energy of the chains, the decrease between 500–530 K is caused by the friction between the chains due to the higher flexibility. The critical slowing

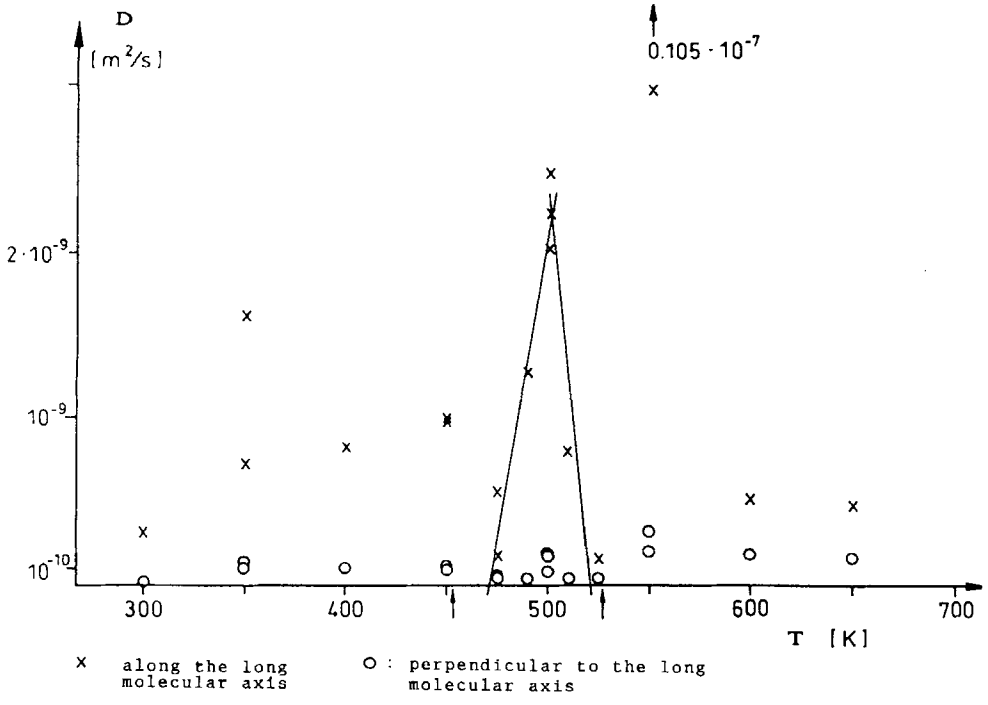

FIGURE 6 Plot of the diffusion constant for the tetramer for different temperatures. These are results from MD-simulations at the density of the nematic phase.

down during the approach towards the crystallisation temperature agrees with the experimental observation of Cheng *et al.*,[18] that thermotropic copolyesters during a transition from the anisotropic melt to the solid state usually pass through aggregation of the rigid chain molecules.

The interpretation of the decrease of translational self diffusion near the isotropisation temperature goes along with the observation of a critical slowing down of the rotational self diffusion with respect to the long molecular axis in Raman and IR-line shape analysis experiments[15] within the nematic phase. The decrease of the rotational selfdiffusion is observed to be accompanied by an increase of the flexibility of the molecules[16] in the nematic phase.

In conclusion we have demonstrated that molecular dynamics simulations on the "all atom level" are useful for the modeling of crystal structures and x-ray powder diagrams. With respect to the simulation of the nematic phase we agree completely with a recently published paper of S. J. Picken, W. F. van Gunstern *et al.*[17]: MD-simulations for liquid crystals depend strongly on the choice and the size of the molecular ensemble and it is clear that one needs to treat a large number of molecules to get reliable results for properties like order parameters and diffusion constants. Also the simulations should be performed much longer than we did. In principle one shall choose fast processes with correlation times within the times scale of $10^{-8} - 10^{-10}$s to be investigated by MD computer experiments. NMR-

measurements are sensitive in the range of $10^{-8} - 10^{+2}$s and with the increasing power of the supercomputers it should be possible to trace conformational changes on the molecular level by molecular dynamics method.

Acknowledgment

We gratefully acknowledge the financial support by the Fond der Chemischen Industrie; this work was performed on an IRIS 4D/70GT work station which was given to us by the above mentioned Fond. The authors also appreciate the support of the Bundesminister für Forschung und Technologie in the frame of the "Materialforschungsprogramm." We thank Prof. G. Wegner for many helpful discussions.

References

1. M. Ballauf, D. Wu, P. J. Flory and E. M. Barral, *Ber. Bunsenges. Phys. Chem.*, **88**, 524 (1984).
2. B. Jung and B. L. Schürmann, *Macromolecules*, **22**, 477 (1989).
3. B. Jung and B. L. Schürmann, *Makromol. Chem., Rapid Commun.*, **10**, 419 (1989).
4. P. Coulter and J. Mooney, Cambridge University, private communication (1989).
5. P. K. Weiner and P. A. Kollmann, *J. Comp. Chem.*, **2**, 287 (1981).
6. H. J. C. Berendsen, J. P. M. Postma, W. F. Van Gunsteren, A. Di Nola and J. R. Haack, *J. Chem. Phys.*, **81**, 3684 (1984).
7. R. W. Hockney and J. W. Eastwood, Computer Simulation using particles (McGraw Hill) (1981).
8. J. M. Adams and S. E. Morsi, *Acta Cryst. B*, **32**, 1345 (1976).
9. P. Coulter, S. Hanna and A. M. Windle, *Liq. Cryst.*, in press.
10. L. E. Alexander, X-Ray Diffraction Methods in Polymer Science, Huntington, N.Y. (1979).
11. A. Einstein, *Ann. Phys.*, **17**, 549 (1905).
12. F. Noak, *Mol. Cryst. Liq. Cryst.*, **113**, 247 (1984).
13. H. Hakemi and M. M. Labes, *J. Chem. Phys.*, **63**, 3708 (1975).
14. S. Nir and W. D. Shain, *Chem. Phys.*, **55**, 1598 (1971).
15. M. P. Fontana, Scriptum of Nato-ASI "The Molecular Dynamics of Liquid Crystals," Il Ciocco, Barga (1989).
16. M. P. Fontana and N. Kirov, *J. Physique Lett.*, **46**, L 341 (1985).
17. S. Picken, W. F. Van Gunsteren, *et al.*, *Liquid Crystals*, **6**, 357 (1989).
18. S. Z. D. Cheng, J. J. Janimak, A. Zhang and Z. Zhon, *Macromolecules*, **22**, 4240 (1989).